Ind. J. Pharm. Edu. Res., 2026; 60(1s):s358-s370.
https://www.ijper.org

Original Article

Unveiling Novel Insights in Chronic Myeloid Leukemia Cell Lines K562 through *in vitro* and *in silico* Approach Targeting of Apoptosis and Oxidative Stress Pathways

Hassan H Almasoudi*

Department of Clinical Laboratory Sciences, College of Applied Medical Sciences, Najran University, Najran, KINGDOM OF SAUDI ARABIA.

ABSTRACT

Introduction: Troxerutin (TR), bioflavanoid derived from rutin posess several biological activity like antioxidant, antinflammatory, antidiabetic and antitumor activity and found to be alternative candidate for cancer therapy. Chronic Myelogenous Leukaemia (CML) is a hematoproliferative disorder caused by uncontrolled myeloid cell division in bone marrow charecterized by Bcr and Abl gene fusion. This study aimed to evaluate the anticancer activity of TR on K562 chronic myeloid leukemia cell line. **Materials and Methods:** The cytoxocity was assessed by MTT and phase contrast microscopy. DAPI staining was carried out to confirm apoptosis. The antioxidant status was determined by Glutathione (GSH) levels. Molecular docking was carried out to understand the interaction between p53 and TR. Caspase-9 level was quantified by ELISA whereas gene expression of BAX, p53 and Bcl-2 level by qRT-PCR. **Results:** The cell growth of K562 was reduced in dose dependent manner with rounding and cell shrinkage. Oxidative stress mediated apoptosis was observed by elevated GSH level and nuclear condensation by DAPI. The increased gene expression level of Bax and p53 with decreased level of Bcl-2 was confirmed. Molecular docking analysis depicted binding affinity of TR with p53 confirming its potential role in apoptosis induction. **Conclusion:** The anticancer activity of troxerutin against K562 cells was induced apoptosis by ROS-mediated oxidative stress and p53-dependent apoptotic pathway supporting therapeutic potential to treat CML.

Keywords: Apoptosis, Caspases, Chronic Myelogenous leukaemia, Flavonoids, *In silico*, Troxerutin.

Correspondence:
Hassan H Almasoudi
Department of Clinical Laboratory Sciences, College of Applied Medical Sciences, Najran University, Najran, KINGDOM OF SAUDI ARABIA.
Email: hhalmasoudi@nu.edu.sa
ORCID: 0000-0002-6722-6667

Received: 22-09-2025;
Revised: 18-11-2025;
Accepted: 01-12-2025.

INTRODUCTION

Chronic Myelogenous Leukaemia (CML), a hematopoietic tissue-related cancer. In a deeper look, CML is characterized by an unchecked growth of haematopoietic progenitors with a distinctive translocation that causes the Abelson (Abl) oncogene to fuse with the Breakpoint Cluster Region (Bcr) gene, commonly referred to as the Philadelphia chromosome.[1] The first line therapeutic option for advanced CML is chemotherapy. Meanwhile, conventional therapeutic methods remain ineffective due to the emergence of drug resistance towards anticancer medications.[2,3] Therefore, there is a need to develop new strategies that increase chemotherapy responsiveness while minimizing adverse effects in cancer patients. Apoptosis is key determinant of cancer pathophysiology, defects in death-signaling pathways allow tumor cells to evade programmed cell death.Hence, inducing the apoptotic pathway of tumour cells is one such efficient therapeutic approach for cancer.[4]

In recent decades, the primary thrust has been on the application of phytochemicals in cancer therapy. Amongst phytonutrient, flavonoids have garnered an excessive amount of attention due to their diverse range of pharmacological properties which includes anti-inflammatory and anti-oxidant properties.[5-7] Troxerutin (TR), a derivative of bioflavonoid rutin, also regarded as Vitamin P4, present in dietary elements, vegetables, and fruits are well recognized for its radical scavenging ability, anti-tumour, anti-thrombotic, anti- fibrinolytic, anti-diabetic, and radio protective attributes, is a subject of significant research interest. Research has demonstrated that TR has anti-mutagenic properties and interacts with DNA and tRNA by means of groove binding and external binding modes. Furthermore, TR has been demonstrated to protect healthy tissues from cancer radiation therapy and to lessen the unfavourable impacts of gamma radiation on cellular DNA. Its efficiency and safety have been reliably shown in older individuals and pregnant women without any adverse reactions.[8-10] Our current study was designed to analyze the anti-tumour efficacy of Tr *in vitro* in human chronic myeloid Leukaemia (K562) cell line as a model additionally, we

DOI: 10.5530/ijper.20263903

assessed *in silico* docking analysis highlights its possible anti-proliferative activity.

MATERIALS AND METHODS

Cell Culture

Human chronic myelogenous leukaemia K562 cell line used in this study was acquired from ATCC. The experiments were conducted between February, 2024 to August, 2024 at xxxxxxx. The K562 cells were maintained and cultured in DMEM (10%) with 2% Pen/Strep antibiotic, incubated in humidified 5% CO_2 at 37°C. Cells were maintained by changing DMEM every 2-3 days until they reached the required confluency and subcultured for further analyses.

Troxerutin preparation

1 mg/mL of Troxerutin (TR) stock was prepared by adding 10 mg of Troxerutin was dissolved in 10 mL sterile distilled water and sterilized using a 0.22 µm syringe and stored at 4°C for the further use.

Cytotoxicity Analysis - MTT Assay

The anti-cancerous ability of TR was validated using MTT assay on K562 cells.[11] Each well of 96 well-plate was seeded with $1x10^5$ cells. Once they attained a confluency of 80-90%, drug was incorporated at the dosages of 200-1000 µg/mL and incubated for 24 hr at appropriate condition. 15 µL of MTT reagent was introduced into well sunder a dark condition and incubated for 4 hr. The Formosan crystal was dissolved by using DMSO (200 µL). The microtiter-plate reader was utilized to read the plate at 490 and 630 nm and the %of inhibition was calculated.

Inhibition (%)=(1- {(OD Treated)490-(OD Treated)630/(OD Control) 490-(OD control)630}×100)

Morphometric Observations

The morphological analysis of control and treated groups was performed. The cells were subjected to 200, 400, and 600 µg/mL of TR and incubated for 24 hr. The culture medium was aspirated, followed by PBS washing of both treated and control cells. The morphological deformations in the treated groups were observed and images were photographed (Phase Contrast microscope, Olympus, Tokyo, Japan).[12]

Fluorescence Assays - DAPI and ROS Staining

The apoptotic potential of TR towards K562 cells was assessed by DAPI staining method. Initially, in 24 well-plate, $1x10^5$ cells were seeded and exposed to different dosages of TR (200-600 µg/mL) for 24 hr. The control and treated groups received a rinse with cooled PBS and exposed to chilled methanol for 10 min. 4% formaldehyde was incorporated for making cells to be permeabilized and DAPI dye (0.5 µg/mL) was utilized for staining the cells. The images were photographed after washing the cells utilizing fluorescence microscope (Nikon, Japan).[13]

The generation of ROS was detected by DCFH-DA method. K562 cells were seeded in 24 well-plate andexposed to dosages (200-600 µg/mL) of TR for 24 hr. Following treatment, both the treated and untreated cells were rinsed with PBS and kept for incubation for 30 min at 37°C with DCFH-DA dye (10 µM). Then, the dye was removed by washing and the photographs were captured using fluorescence microscope.[14]

Determination of Antioxidant Marker - Reduced Glutathione (GSH) Analysis

The reduced glutathione assay was carried out as per the protocol mentioned by Goh *et al*., 2011[15] with minor alterations. After trypsinization and centrifugation, the pellets were homogenized in 0.1 M potassium phosphate buffer; the buffer pH was adjusted to 7.4. An equivalent volume of 4% sulfo salicyclic acid was added to 0.5 mL of homogenate, and the mixture was incubated for 1hr at 4°C. The suspension obtained was centrifuged and 0.03 mL of supernatant was taken, to that 0.9 mL of 0.1 M Potassium phosphate buffer, 0.066 mL of DTNB were added. The absorbance was read at 412 nm. The reduced glutathione was expressed in terms of mM.

Analysis of Caspase Activity and Gene Expression Studies

Caspase 9 plays main role in apoptotic signalling cascade. The activity of caspase 9 was determined by colorimetric test kit (Elabscience, US). The experiment performed based on the manufacturer's protocol.[16] $1x10^4$ cells/well were seeded in 96 well-plate. After attaining the desired confluency, the cells were subjected to drug at the dosages of 200-600µg/mL for 24 hr. Using ice-cold phosphate buffer saline, the treated and untreated cells were homogenized and centrifuged to collect cell lysate. 30 µL of cell lysate was added to 20 µL of caspase-9 substrate (Ac-LEHD-pNA), and 150 µL of reaction buffer was mixed to it, and incubated for 15 min. Using an ELISA reader (ELX-800n, Biotek, USA), the fluorescence of the reaction mixture was monitored for 15 min at 5 min intervals and the absorbance was recorded at 430 and 535 nm. The final results were normalized with untreated cell control.

qPCR was used to assess the expression levels of apoptotic markers (p53, Bax) and the anti-apoptotic gene Bcl-2. Total RNA was isolated using RNAiso Plus (Takara, Cat. No. 9108), and RNA integrity was verified by agarose gel electrophoresis. A total of 2 µg RNA was used for cDNA synthesis with the cDNA Synthesis Kit (Takara, Cat. No. 6110A). Real-time PCR was performed using the TB Green Premix Ex Taq II master mix (Takara, Cat. No. RR820A). Each 20 µL reaction contained 2 µL cDNA, 10 µL TB Green Master Mix, 1 µL forward primer, 1 µL reverse primer (Table 1), and 6 µL RNase-free water.

PCR amplification was carried out for 40 cycles with the following thermal profile: initial denaturation at 95°C for 3 min; denaturation at 95°C for 15 sec; annealing at 54.2°C; and extension at 72°C for 30 sec. All reactions were run in triplicate in a 96-well plate on the Bio-Rad CFX96 Real-Time System (Bio-Rad Laboratories, USA).

Relative mRNA expression was calculated using the $2^{-\Delta\Delta Ct}$ method, based on Ct values of target and reference genes. β-actin served as the internal control. Amplicon specificity was confirmed by melt-curve analysis (single peak) and by agarose gel electrophoresis to verify product size and absence of non-specific bands.

In silico Docking Assessment

Acquisition of 3D Structures of Protein and Ligand

The Three-Dimensional (3D) structure of the ligand TR was retrieved in SDF format from the PubChem database (CID: 5486699). The structure was converted to PDBQT format using AutoDock Tools (MGLTools) for compatibility with molecular docking software. The crystal structure of the *p53* tumor suppressor protein was retrieved from the Protein Data Bank (PDB) with the ID 2J21. Water molecules, heteroatoms, and non-standard residues were eliminated from the protein structure prior to docking. Hydrogen atoms were infused, and Gasteiger charges were were allocated. The processed structures were employed for docking simulations.

Molecular Docking

Molecular docking was employed to figure out the binding affinity and interaction profile of TR and *p53*. The prepared PDBQT files of the ligand and receptor were imported into H-Dock software. The docking grid box was configured with free pockets that covered the active site region of *p53*. Docking calculations were carried out using H-Dock. The most desirable binding poses were elected according to the binding affinity, confidence, and interaction profiles. The binding interactions were further visualized and analyzed using BIOVIA Discovery Studio Visualizer 2024 R2. The H-dock applies a knowledge-based iterative scoring system. Higher negative docking scores indicate a more likely binding model.

Lipinski's Rule of Five

TR's drug-likeness was assessed using Lipinski's Rule of Five, which takes into account essential physicochemical traits such as molecular weight, hydrogen bond donors/acceptors, and Lipophilicity (log P). The evaluation was carried out employing the SwissADME online application (https://www.swissadme.ch).

Drug-Likeness and Prediction of Toxicity

Examination of drug-likeness and toxicity aspects is critical in establishing a chemical compound's capability as an oral medication. These were analysed implementing ADMET lab 2.0. This tool imparts data pertaining to potential mutagenic, tumorigenic, reproductive, and irritating effects based on chemical structure and functional groups.

Bioactivity Score

The bioactivity score of TR was computed using SwissADME. The score predicts the compound's interaction with common therapeutic targets (e.g., GPCRs, enzymes, and ion channels). High activity is marked by scores greater than 0.00, moderate activity by scores between -0.50 and 0.00, and inactivity by values less than -0.50.

ADMET Analysis

ADMET profiling (Absorption, Distribution, Metabolism, Excretion, and Toxicity) was accomplished using ADMETlab 2.0 (https://admetmesh.scbdd.com). Parameters assessed included:

- **Absorption:** Gastrointestinal (GI) absorption and Caco-2 permeability,
- **Distribution:** Blood-brain barrier (BBB) penetration,
- **Metabolism:** Cytochrome P450 enzyme interactions,
- **Excretion:** Renal and biliary clearance predictions,
- **Toxicity:** Hepatotoxicity, cardiotoxicity, and overall safety.

Statistical analysis

GraphPad Prism of version 8.1 was employed for statistical analysis. The experiments were carried out as triplicates and findings were computed employing one-way ANOVA. Tukey's multiple comparison test was applied to compare treated and control cells. Data are denoted as Mean±SD. $p<0.05$ was taken as significant.

RESULTS

Cytotoxicity Analysis - MTT Assay

The cytotoxic ability of TR on K562 cells was assessed employing the MTT assay. The IC_{50} value was determined to be 400 µg/mL corresponding to 45.85% inhibition of cell viability. The highest tested concentration (1000 µg/mL) resulted in 95.87% inhibition. 200 µg/mL of TR showed moderate significance with the untreated cells with ** indicating $p<0.001$ while the other dosages 400, 600, 800 and 1000 µg/mL showed the high significance with the control group as *** indicating $p<0.0001$. As illustrated in Figure 1, TR exhibited a dose-dependent cytotoxic response with cell viability progressively decreasing with increasing concentrations. These MTT assay results provide preliminary evidence of the potent anti-cancer activity of TR against K562 cells.

Morphometric Observations

The morphological examination of the treated cells is another important factor for assessing the antiproliferation effect of TR (200-600 µg/mL) on K562 cells. Compared to the control cells, the treated cells showed more detached cells. Additionally, as Figure 2 illustrates, there are noticeable morphological alterations, including cell blebbing, disoriented cells, shrinkage and rupturing of cells especially in the drug-treated groups.

Fluorescence Assays - DAPI and ROS Staining

In DAPI Staining, the dose-responsive rise in blue fluorescence cells, which shows that TR has cytotoxic effects on K562 cells as represented in Figure 3. Condensed nuclei and chromatin disruption were observed in the treated cells. Untreated cells, on the other hand, displayed their normal cell structure devoid of any abnormalities. The photomicrographs of ROS staining revealed as compared to control cells, TR-treated cells resulted in enhanced DCF-fluorescence (green colour) intensity in K562 cells showing an elevated intracellular ROS levels. The images are depicted in Figure 4.

Determination of Antioxidant Marker - Reduced Glutathione (GSH) Analysis

The GSH assay revealed a dose related decrease in glutathione levels in TR-treated K562 cells on comparison with the control cells (Figure 5). At dosages of 200, 400, and 600 µg/mL, the GSH levels were measured at 0.261±0.011, 0.204±0.018, and 0.050±0.011 mM/mL of sulfhydryl units, respectively. Statistical interpretation exhibits $p<0.01$ (*), $p<0.001$ (**) and $p<0.0001$ (***) for TR 200, 400 and 600 µg/mL respectively compared to control group demonstrating the significant reduction of GSH level. This reduction in intracellular GSH indicates enhanced oxidative stress, supporting the potent anti-cancer activity of TR against K562 cells.

Analysis of Caspase Activity and Gene Expression Studies

The caspase pathway is well known to be one of the main processes behind apoptosis and cell death. Figure 6 illustrates that dose-dependent elevation in the level of caspase-9 in treated groups on comparing with the control group and also showed the high significance with as $p<0.0001$ with ***. The caspase-9 results showed that TR triggers caspase pathways, which causes K652 cells to undergo apoptosis.

The levels of apoptotic and anti-apoptotic markers were studied in order to understand the molecular changes in K562 cells after TR treatment, as shown in Figures 7-9. In contrast to the control group, the levels of *Bcl-2* declined in the treated groups. 200 µg/mL group showed non-significance ($p>0.05$) with control group whereas 400 and 600 µg/mL groups showed high significance ($p<0.0001$). Conversely, TR-treated groups exhibited elevated levels of apoptotic markers, specifically *Bax* and*p53*, at the dosages of 200, 400, and 600 µg/mL. Statistical analysis of BAX gene expression indicated that 200 and 400 µg/mL showed low significance with untreated group with * - $p<0.05$ and 600 µg/mL group showed the moderate significance with control group

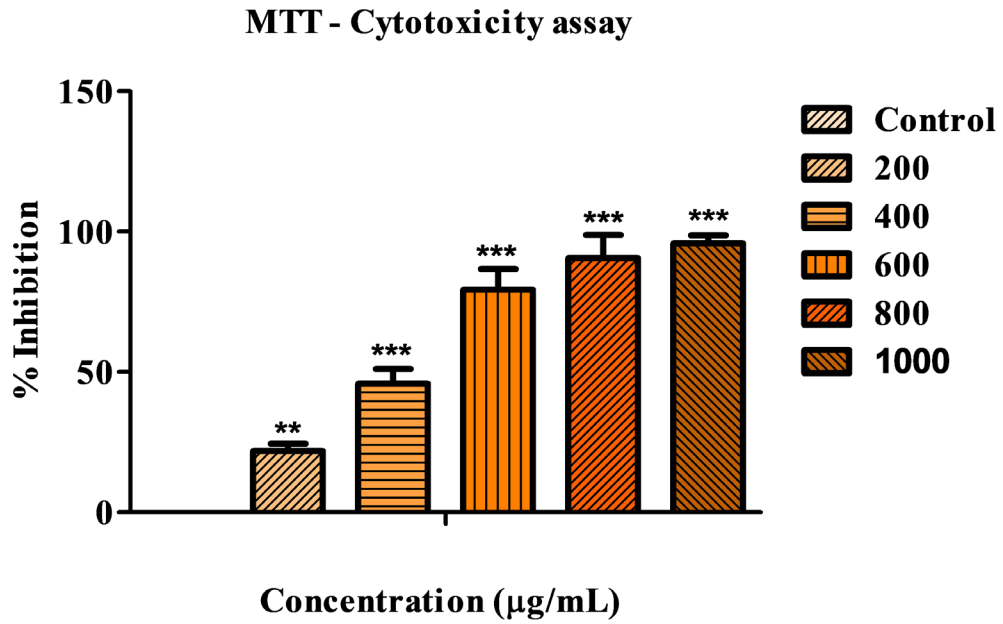

Figure 1: MTT Assay. Cytotoxic studies. Cytotoxic effect of TR on K562 cells evaluated by MTT assay. The figure illustrates the concentration-dependent inhibition of cell viability, with the 45.85% inhibition observed at 400 µg/mL.

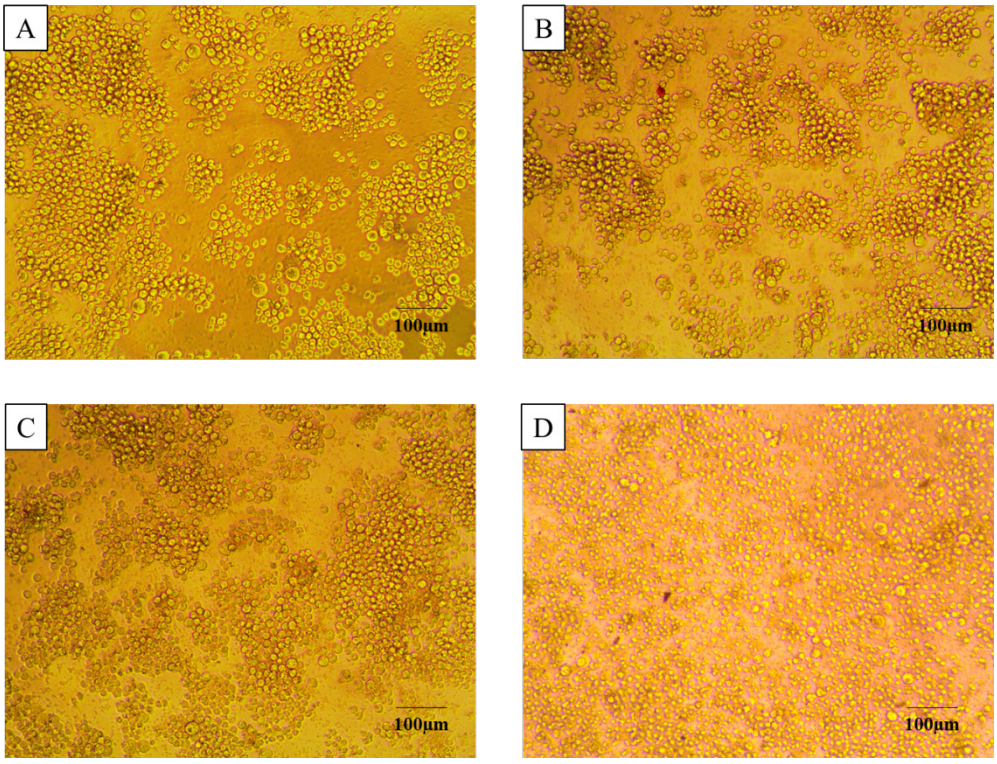

Figure 2: Morphological analysis. Morphological evaluation of K562 cells with TR treatment. (A) represents the control group showing normal cellular morphology, while (B-D) shows treated cells exposed to increasing concentrations (200-600 µg/mL) of the test compound, exhibiting prominent dose-dependent morphological deformations. Images were captured under an inverted microscope at 20x.

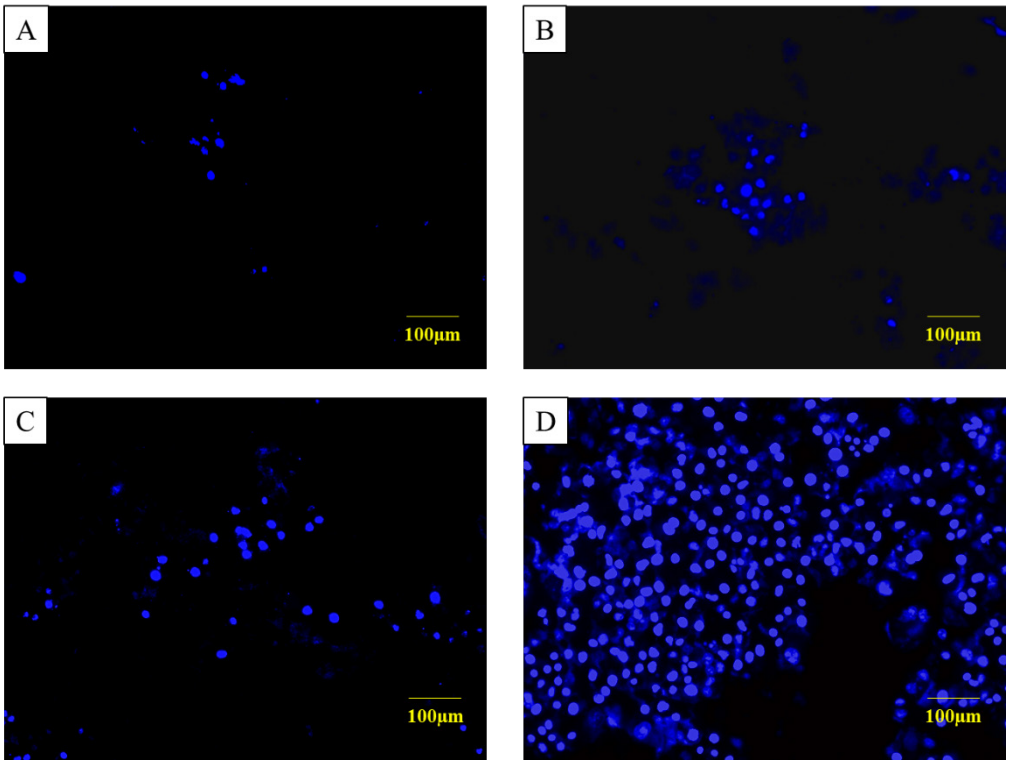

Figure 3: DAPI staining. DAPI staining of K562 cells to assess nuclear morphology upon treated with TR. Representative fluorescence microscopic images show (A) control cells with uniform, intact nuclei and (B-D) TR-treated cells (200-600 µg/mL) displaying condensed and fragmented nuclei, characteristic of apoptotic changes. Blue fluorescence indicates DAPI-stained nuclei.

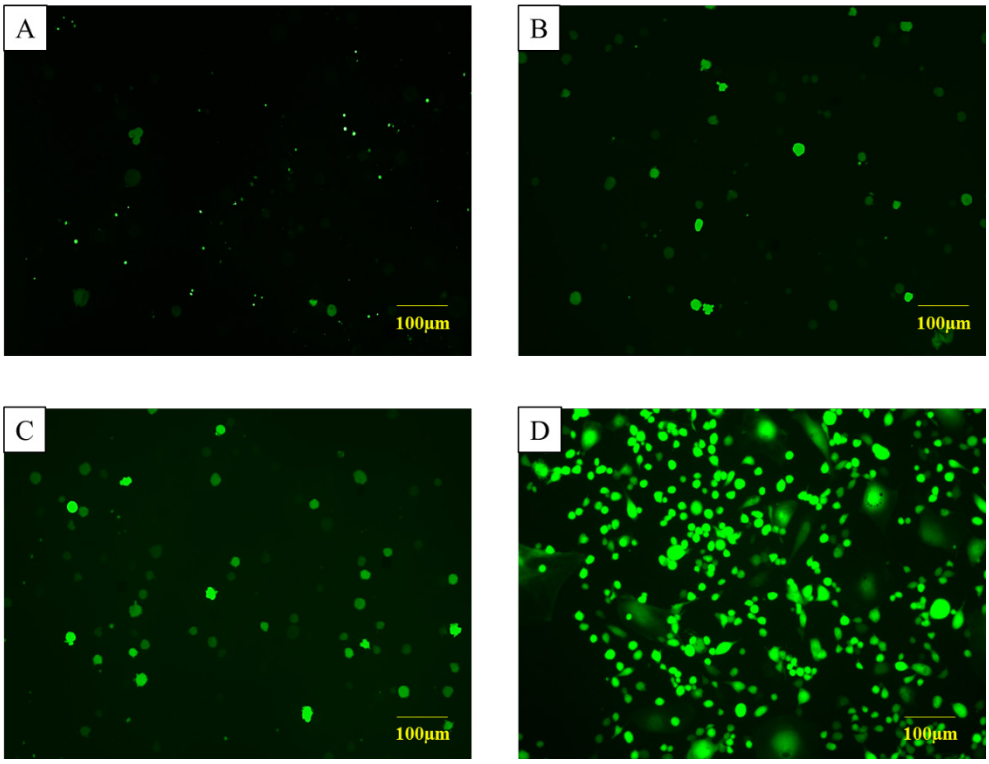

Figure 4: ROS staining. ROS staining of K562 cells following TR treatment. Representative fluorescence microscopic images illustrate (A) control cells with low ROS levels and (B-D) TR-treated cells (200-600 µg/mL) showing enhanced green fluorescence, confirming increased intracellular ROS generation in a dose-dependent pattern.

Table 1: Primers list. List of primers used for real-time PCR analysis. The table presents the forward and reverse primer sequences of the target genes used in quantitative real-time PCR (qRT-PCR) experiments to evaluate gene expression levels in K562 cells.

Sl. No.	Gene	Oligo nucleotides	Temp.
1	Beta-actin	GCAGATGTGGATCAGCAAGC GCAGCTCAGTAACAGTCCGC	54.2
2	Bcl-2	TACCTGAACCGGCACCTG GCCGTACAGTTCCACAAAGG	54.2
3	Bax	CCTGCTTCTTTCTTCATCGG AGGTGCCTGGACTCTTGGGT	54.2
4	p53	CTCTGACTGTACCACCATGG CCGTCCCAGTAGATTACCAC	54.2

as ** - p<0.01. Similarly, 200 and 400 µg/mL group in p53 gene expression indicated the same as BAX gene demonstrating low significance with untreated control group with * - p<0.05 whereas 600 µg/mL showed high level of significance with control group with **** - p<0.0001. The gene expression study confirming the supportive apoptotic and anti-apoptotic gene expression outputs.

In silico Docking Assessment

Molecular Docking

The docking analysis revealed that TR effectively binds to *p53* (PDB ID: 2J21) with a H-Dock binding score affinity of -212.90 with a confidence score of 0.7877, revealing a strong interaction with *p53*. At the protein's binding pocket, visualization of the docking complex showed both hydrophobic and hydrogen bonding interactions. These interactions imply that TR could be able to alter the biological functions of *p53*. (Figures 10-13).

Analysis of Lipinski's Rule of Five

The Topological Polar Surface Area (TPSA) was found to be 297.12 Å^2. According to Lipinski's Rule of five, TR exhibited three violations (molecular weight > 500, high TPSA, and number of hydrogen bond donors). The values are represented in Table 2.

Prediction of Toxicity

TR demonstrated no acute toxicity or genomic carcinogenicity risks identified by ADMETlab2.0 with slight aquatic toxicity effect alert.

Bioactivity Score

TR demonstrated a bioactivity score of 0.17, suggestive of average pharmacological efficacy

and highlights its potential as a lead compound for *p53*-targeting therapeutic development.

ADMET Analysis

ADMET analysis showed that TR may pass into the host metabolic system without causing any adverse effects. Additionally, TR showed low GI absorption with negative to the penetration of Blood-brain barrier. (Table 2).

DISCUSSION

A myeloproliferative neoplasm referred to as Chronic Myelogenous Leukaemia (CML) is caused by a constitutively active tyrosine kinase called Bcr-Abl, which is produced by an oncogene that originates from a complementary displacement between 9 and 22 chromosomes. The annual incidence of CML, a rare haematologic cancer, ranges from 1.0 to 1.5/10^5, and has no

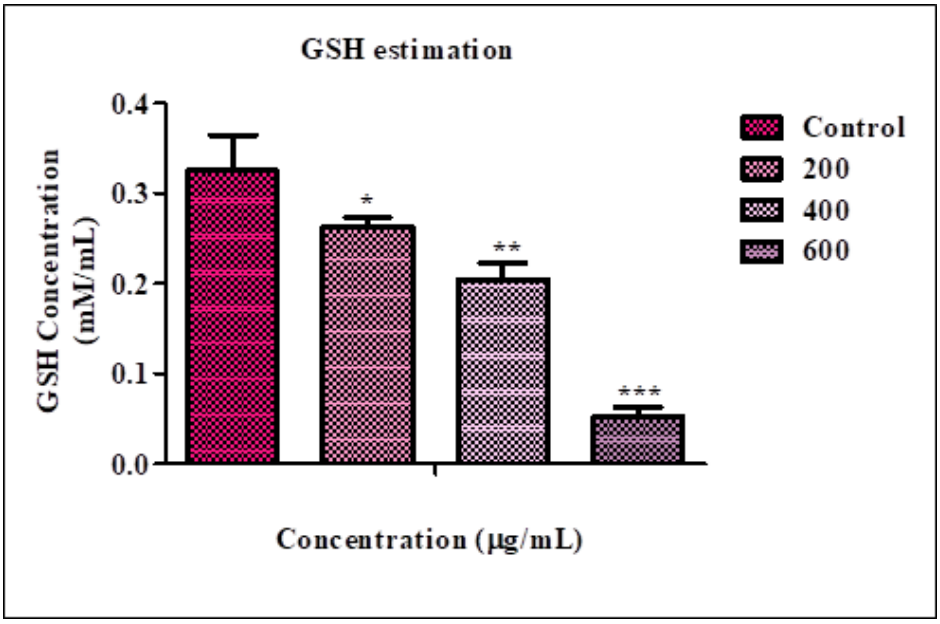

Figure 5: GSH assay. Estimation of intracellular glutathione (GSH) levels in K562 cells. The bar graph represents GSH levels in control and TR-treated groups. Reduction in GSH was noticed in treated groups compared to control, indicating oxidative stress induction.

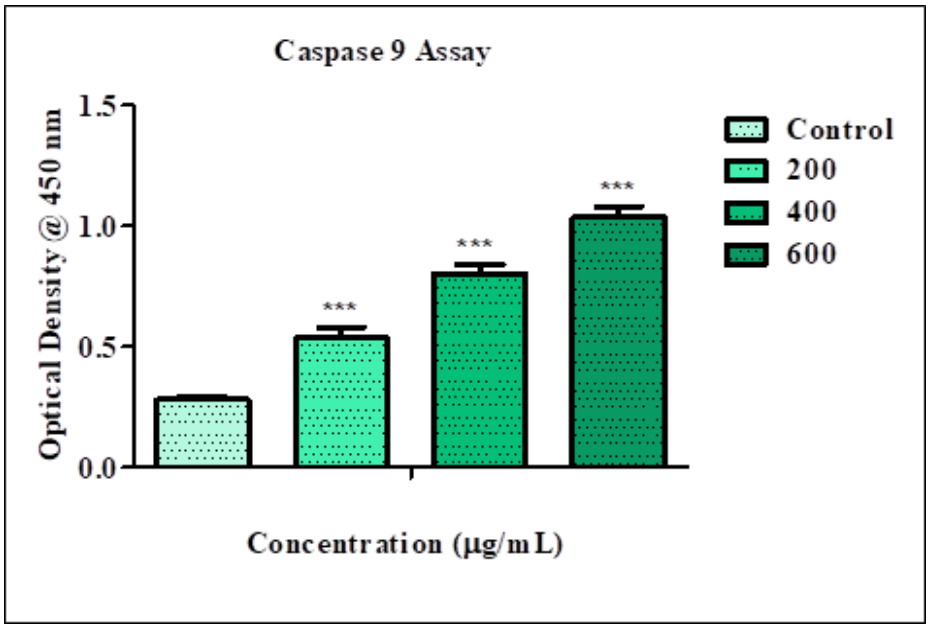

Figure 6: Caspase-9. Evaluation of caspase-9 activity in K562 cells. The graph illustrates a significant elevation in caspase-9 activity in TR-treated groups compared to the control, indicating activation of the intrinsic apoptotic pathway.

Table 2: Lipinski's rule and ADMET scores. Lipinski's Rule of Five and ADMET analysis of TR. The table represents the physicochemical parameters of TR based on Lipinski's Rule of Five along with that ADMET (Absorption, Distribution, Metabolism, Excretion, and Toxicity) scores were calculated and indicating its drug-likeness and pharmacokinetic properties.

Lipinski's Rule of Five								
Topological Polar Surface Area (Å)	c logP (<5)	MW (<500)	Heavy atom count (natoms)	Hydrogen bond donors (nOHNH) (≤5)	Hydrogen bond acceptors (nON) (≤10)	Rotatable bonds (nrotb) (≤10)	Lipinski Violations	
297.12	2.64	742.68	52	10	19	15	3	
ADMET								
Consensus Log Po/w	BBB	P-gp Substrate	CYP1A2 inhibitor	CYP2C19 inhibitor	CYP2C9 inhibitor	CYP2D6 inhibitor	CYP3A4 inhibitor	Log Kp
-1.47	No	No	No	No	No	No	No	-11.83 cm/s

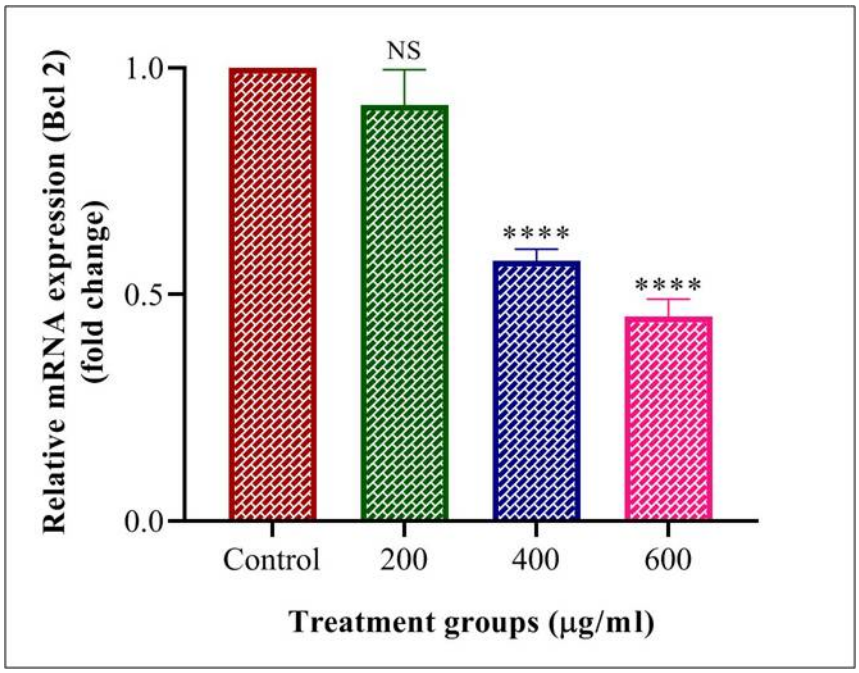

Figure 7: Gene expression studies on Bcl-2. Effect of TR on Bcl-2 gene expression in K562 cells. The graph represents the relative expression levels of Bcl-2 in control and TR-treated groups. A marked downregulation of Bcl-2 was observed in the treated groups than control group, indicating induction of apoptosis. Mean±SD (n=3) values were provided. One-way ANOVA followed by Tukey's multiple comparison test was used. ****p<0.0001, ***p<0.001, **p<0.01, *p<0.05, and NS - Non-significant. * Indicates comparison between control and treated groups.

significant variation in incidence by race or geography. Tyrosine Kinase Inhibitors (TKIs) of Bcr-Abl1 redefined the therapy of CML and marked the age of targeted anti-cancer medications. Since the approval of three successive generations of Bcr-Abl1 TKIs, most CML patients now have long-term remissions and nearly normal life expectancies.[17,18] Despite the effectiveness of TKIs in chronic-phase CML, resistance can develop in a subset of patients leading to disease progression into blast crisis. Blast phase-CML is associated with poor prognosis, therapeutic resistance, and frequent relapse. Therefore, even with TKIs as standard therapy, alternative or adjunct strategies are still required.[19] Combating TKIs resistance, introducing alternative anti-cancer drugs, and enhancing the prognosis of blast phase-CML are current research horizons in the field of CML therapy.[3]

Phytonutrients are capturing a lot of attention in a quest for novel, lower-toxic, and more curative chemo preventive and anti-tumor medications.[20] Notably, flavonoids play a significant role in the biomedical field with their wide array of biological and therapeutic properties, affordability, accessibility, with excellent tolerance.[21-23] Troxerutin (TR), a natural derivative of bioflavonoid rutin, is one such phytocompound.[24] The anti-cancer properties of TR towards K562 cells are the focus of our current study. There is only minimal research regarding *in silico* studies found in the

K562 cell line; hence, we also explored TR's interaction with *p53* gene (tumor -suppressor).

The outcomes of the MTT assay revealed higher dosage of TR exhibited excellent cytotoxicity, demonstrating 95% of inhibition against K562 cells.[24] Our morphometric photographs of control and drug-treated cells further confirmed the anti-proliferative efficacy of TR. The nuclear condensation, shrinkage, and rounded cells were observed in the treated groups. In DAPI staining, the blue fluorescence cells were predominantly found in a dose-related trend, signifying the condensed nuclei. ROS staining makes it evident that a considerable quantity of free radicals was released, as evidenced by the dose-dependent increase in green fluorescence, which disclosed that the cytotoxic activity was elevated. The phytocompounds exhibit a wide array of anticancer strategies, including altering the activities of ROS-scavenging enzymes, triggering apoptosis, autophagy, reducing the proliferation and invasiveness of cancer-causing cells.[5,25] The levels of antioxidants, GSH was declined in treated groups suggests that redox equilibrium is hampered.[26] So far, from the findings of our study it was evidenced that TR demonstrated anti-tumor ability in K562 cells via inducing apoptosis. The development of resistance to existing anti-cancer drugs in CML has detrimental effects, as previously stated. Consequently, novel apoptosis inducers could potentially be a new therapeutic strategy specifically in case of CML. Our current research addressed this aspect, demonstrating that TR trigger apoptosis and function as a powerful anti-cancer medication.

To further confirm the cytotoxic effect of TR on K562 cells through the induction of apoptosis, we evaluated the activity of caspase-9 along with the levels of prominent apoptotic and anti-apoptotic markers. Apoptosis is governed via intrinsic (mitochondrial) and extrinsic (death receptor-mediated) pathways. The mitochondrial mediated pathway is initiated by internal cellular stress, leading to mitochondrial dysfunction and subsequent activation of caspases. The extrinsic pathway, on the other hand, is prompted by the engagement of pro-apoptotic cell surface receptors, culminating in caspase activation. Caspase-3 functions as a critical executioner in both pathways, further activating caspases-8 and -9.[27] In our study, TR-treated cells exhibited upregulated expression of caspase-9, suggesting that TR induces apoptosis primarily via the intrinsic pathway. This effect appears to result from TR-mediated disruption of the mitochondrial membrane potential, coupled with reduced regulation of the Bcl-2 and overexpression of Bax, Cytochrome c, Caspase-9, and Caspase-3. The elevation in the Bax/Bcl-2 ratio is a well-established hallmark of mitochondrial-dependent apoptosis. Our results demonstrated a significant downregulation of Bcl-2 along with elevated expression of Bax and p53, underscoring the pivotal role of the Bcl-2 family in TR-induced apoptosis in K562 cells. Notably, Bcl-2 functions to inhibit apoptosis by preventing the release of mitochondrial apoptogenic factors, potentially through interaction with mitochondrial porin channels. In contrast, p53 acts as a tumor suppressor that halts abnormal cell proliferation under cellular stress and DNA

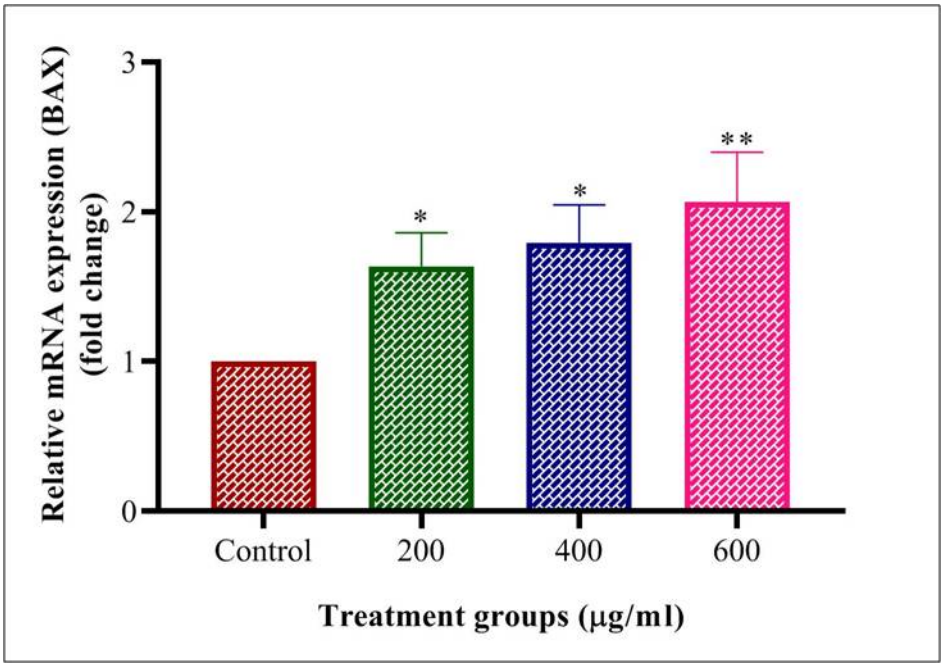

Figure 8: Gene expression studies on Bax. Effect of TR on the expression of Bax in K562 cells. The graph represents the relative expression levels of Bax in control and TR-treated groups. A significant upregulation of Bax expression was observed in the treated groups than the untreated group, confirming activation of the apoptotic pathway. Data are expressed as mean±SD (*n*=3). One-way ANOVA followed by Tukey's multiple comparison test was used. ****$p<0.0001$, ***$p<0.001$, **$p<0.01$, *$p<0.05$, and NS - Non-significant. * - Denotes comparison between control and treated groups.

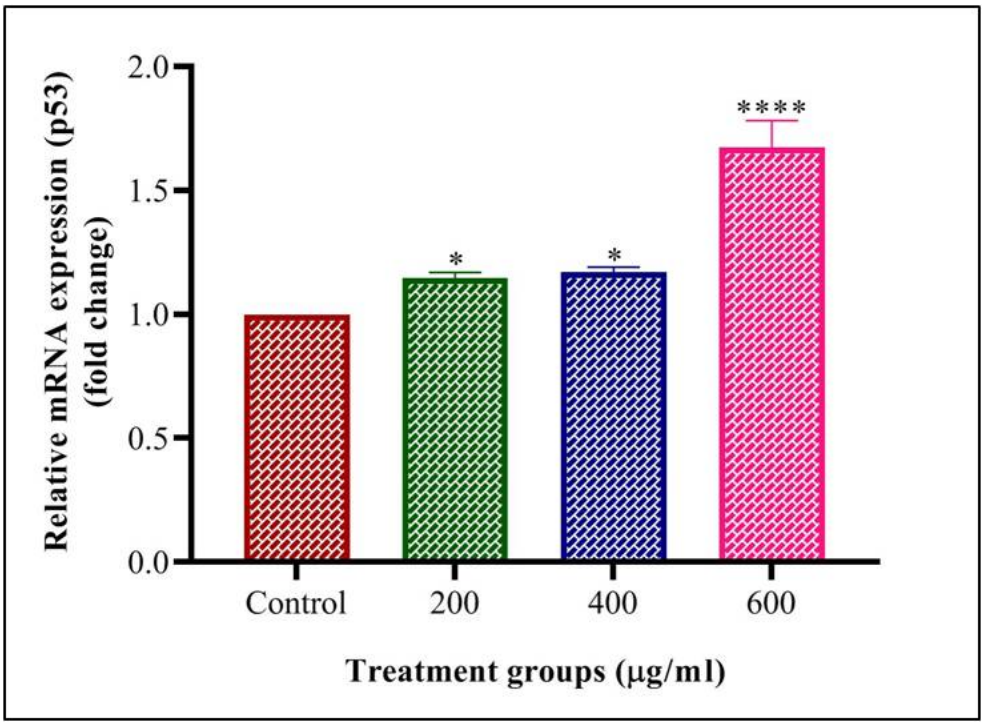

Figure 9: Gene expression studies on p53. Effect of TR on p53 gene expression in K562 cells. The graph illustrates the relative mRNA expression levels of p53 in control and TR-treated groups. Gradual upregulation of p53 expression was noticed in the treated groups compared to the control, indicating activation of p53-mediated apoptotic signalling. One-way ANOVA followed by Tukey's multiple comparison test were used. ****$p<0.0001$, ***$p<0.001$, **$p<0.01$, *$p<0.05$, and NS - Non-significant. * - Denotes comparison between control and treated groups.

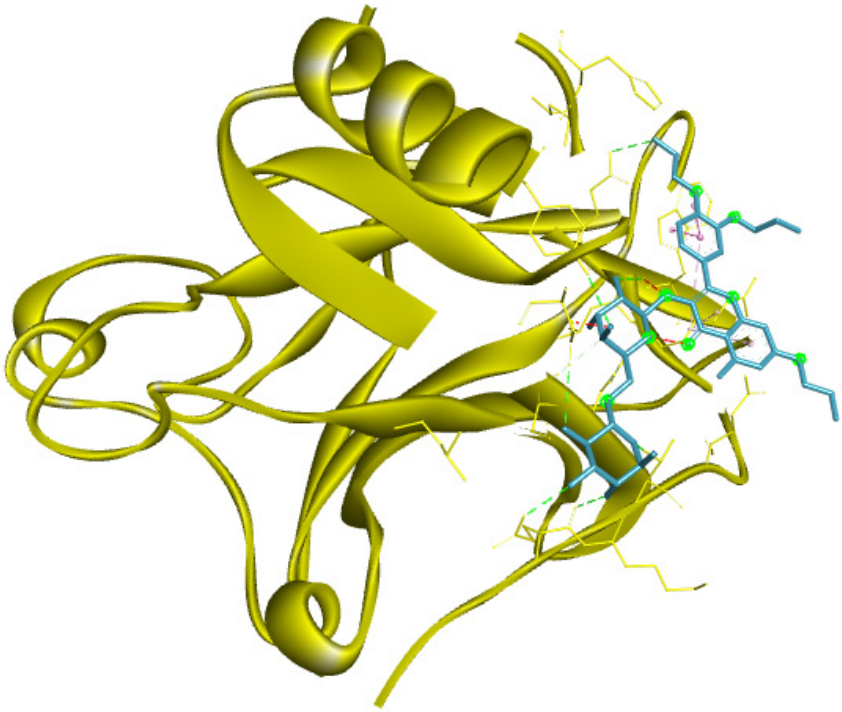

Figure 10: *In silico* studies - Molecular interaction. Molecular docking interaction of TR with p53. The figure depicts the docked complex of TR bound to the p53 protein, illustrating the binding orientation within the active site. The interaction exhibited a binding interaction as −212.90, indicating strong binding score between TR and p53.

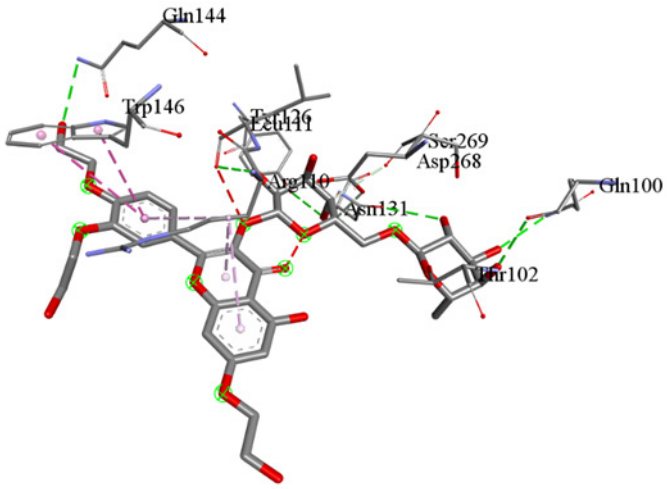

Figure 11: Ligand interaction diagram of TR with p53 protein. The figure illustrates the detailed molecular interactions within the binding pocket, highlighting the formation of H-bonds and hydrophobic contacts between TR and main amino acid residues of the p53 protein.

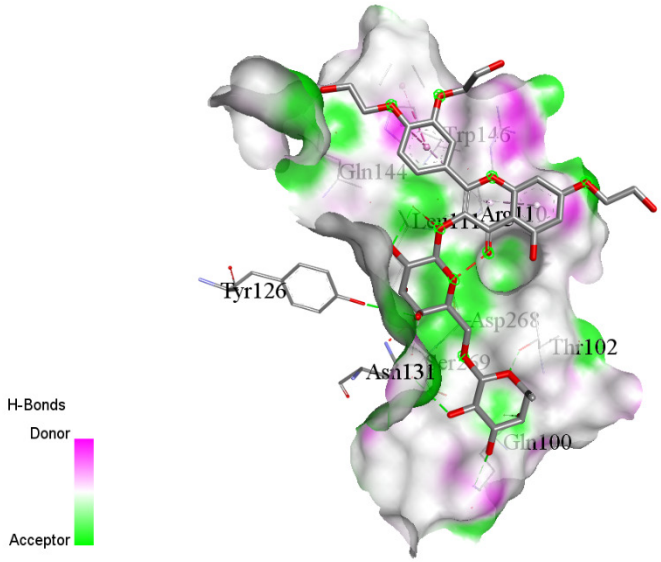

Figure 12: 3D image of interaction. Three-dimensional H- donor and acceptor map of the TR-p53 complex. The figure represents the spatial positioning of H-bond donor and acceptor regions within the binding pocket, illustrating the interaction pattern that stabilizes the TR-p53 complex.

damage, thereby promoting apoptosis. Overexpression of p53 in TR-treated cells further supports its involvement in the apoptotic process triggered by TR.[4,28-31] Collectively, our findings of *in vitro* studies showed that TR could block the event of tumorigenesis via shifting *Bax/Bcl-2* ratio, and activation of caspases. This was in accordance with otherreports, stating, flavonoids have the ability to raise the levels of activated caspases-3, 8, and 9, which causes leukaemia cells to undergo apoptosis. Jalal *et al.*, 2020 stated that Troxerutin up-regulated the expression of *Bax* which leads to cleavage of caspase-3 ultimately ends up in apoptosis in HeLa cells.[24]

In order to further establish the TR's cytotoxic capability, *in silico* docking analysis were performed. *In silico* docking study was conducted using HDOCK, a semi-automated docking tool that employs hybrid template dependent or independent docking strategy. It uses complex algorithm to define grid parameters and identify active sites in the protein. The statistical algorithm of HDOCK gives a binding score along with its statistical confidence,

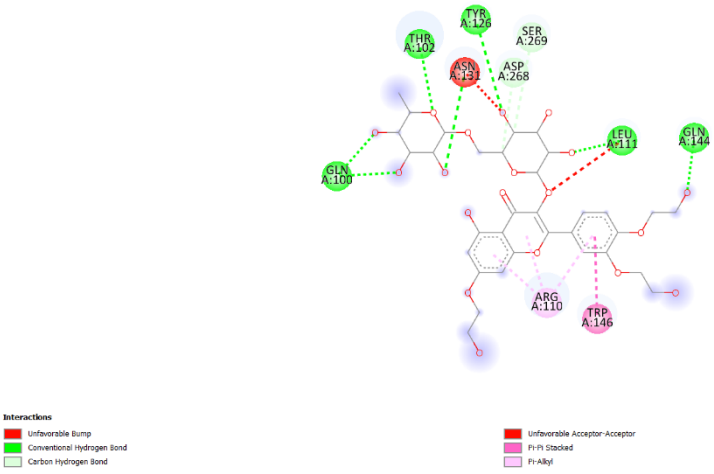

Figure 13: Chemical structure interaction. Two-dimensional chemical structure representation of the TR-p53 complex. The figure demonstrates the 2D interaction pattern of the TR-p53 complex, depicting the arrangement of functional groups and their bonding interactions within the molecular framework.

indicating the favourability of protein-ligand binding conditions. TR has a favourable binding condition with the *p53* tumour suppressor protein, as identified by the highly favourable H DOCK docking score of 212.9.[32] This suggests that TR may modulate its regulatory function, particularly in the pathways associating in the response to cellular stress and DNA damage. The highly favourable interaction condition as per docking analysis and the occurrence of both polar and non-polar interactions claims its capability to stabilize *p53* conformation or possibly obstruct its degradation pathways. These results provide compelling evidence that TR can interact with *p53*. Besides, comprehensive metabolic and drug likelihood investigations provide additional perspective on TR's potential as a medication that doesn't interfere with the host's biochemical and metabolic processes. Despite violating certain criteria of Lipinski's Rule of Five, TR is still a viable lead because of its favourable bioactivity and manageable toxicity profiles. The ADMET profile exhibits adequate safety with no significant red flags of mutagenicity or hepatotoxicity, regardless of limits in absorption and blood-brain barrier penetration. For hematological malignancies like CML, systemic circulation and hepatic metabolism are of greater significance than BBB penetration. Therefore, while low BBB permeability is observed, it does not negatively impact the therapeutic feasibility of Troxerutin for CML treatment. Additionally, no acute toxicity or genomic carcinogenicity were found making TR as a potent anti-cancer drug. This computational investigation supports earlier research on the possible therapeutic benefits of polyphenols and natural flavonoids in cancer signalling pathways. TR's strong interaction with *p53*merits additional *in vitro* and *in vivo* research to confirm its mode of action and drug-likeness, which could lead to its development as an anticancer medication that targets *p53*-dependent pathways. Hence, the outcomes of our present study clearly implied that TR's potent effect on inhibiting the K562 cells proliferation through apoptosis induction, it is translation to chemotherapeutic application requires further *in vivo* validation and comparative efficacy studies.

CONCLUSION

Troxerutin (TR) reduced K562 cell viability, increased ROS, decreased GSH, and elevated caspase-9 activity, confirming intrinsic apoptotic pathway activation. The upregulation of p53 and Bax along with downregulation of Bcl-2 further supports caspase-9-mediated apoptosis. Molecular docking also indicates interaction between TR and p53 confirming strengthening the mechanistic interpretation. Although findings highlight TR as a promising candidate for CML therapy, further *in vivo* validation and comparative efficacy studies are required before clinical translation.

ACKNOWLEDGEMENT

The authors are thankful to the Deanship of Graduate Studies and Scientific Research at Najran University for funding this work under the Easy Funding Program grant code (NU/EFP/MRC/13/216).

ABBREVIATIONS

TR: Troxerutin; **CML:** Chronic Myelogenous Leukemia; **ROS:** Reactive Oxygen Species; **GSH:** Glutathione; **PCR:** Polymerase Chain Reaction; **DAPI:** 4,6-Diamidino-2-Phenylindole; **DCFH-DA:** 2,7-Dihydrofluroscein Diacetate; **FBS:** Fetal Bovine Serum; **TPSA:** Topological Polar Surface Area; **MTT:** 3-(4,5-Dimethyl-2-Thiazolyl)-2,5-Diphenyltetrazolium Bromide; **DMEM:** Dulbecco's Modified Eagle Medium.

CONFLICT OF INTEREST

The authors declare that there is no conflict of interest.

FUNDING

This research was funded by the Najran University under Easy Funding Program with grant code NU/EFP/MRC/13/216.

REFERENCES

1. Verma D, Kantarjian HM, Jones D, Luthra R, Borthakur G, Verstovsek S, *et al.* Chronic myeloid leukemia (CML) with P190BCR-ABL: analysis of characteristics, outcomes, and prognostic significance. Blood. 2009;114(11):2232-5. doi: 10.1182/blood-2009-02-204693.
2. Dawson A, Zarou MM, Prasad B, Bittencourt-Silvestre J, Zerbst D, Himonas E, *et al.* Leukaemia exposure alters the transcriptional profile and function of BCR:ABL1 negative macrophages in the bone marrow niche. Nat Commun. 2024;15(1):1090. doi: 10.1038/s41467-024-45471-0, PMID 38316788.
3. Osman AE, Deininger MW. Chronic myeloid leukemia: modern therapies, current challenges and future directions. Blood Rev [Internet]. 2021;49:100825. doi: 10.1016/j.blre.2021.100825, PMID 33773846.
4. Chun-Guang W, Jun-Qing Y, Bei-Zhong L, Dan-Ting J, Chong W, Liang Z, *et al.* Anti-tumor activity of emodin against human chronic myelocytic leukemia K562 cell lines *in vitro* and *in vivo*. Eur J Pharmacol [Internet]. 2010 Feb 10;627(1-3): 33-41. doi: 10.1016/j.ejphar.2009.10.035, PMID 19857484.
5. Kopustinskiene DM, Jakstas V, Savickas A, Bernatoniene J. Flavonoids as anticancer agents. Nutrients. 2020;12(2):457. doi: 10.3390/nu12020457, PMID 32059369.
6. Almasoudi HH, Saeed Jan M, Nahari MH, Alhazmi AY, Binshaya AS, Abdulaziz O, *et al.* Phenolic phytochemistry, *in vitro, in silico, in vivo*, and mechanistic anti-inflammatory and antioxidant evaluations of Habenaria digitata. Front Pharmacol [Internet]. 2024;15:1346526. doi: 10.3389/fphar.2024.1346526, PMID 38487169.
7. Rodríguez-García C, Sánchez-Quesada C, Gaforio JJ, Gaforio JJ. Dietary flavonoids as cancer chemopreventive agents: an updated review of human studies. Antioxidants (Basel). 2019;8(5):137. doi: 10.3390/antiox8050137, PMID 31109072.
8. Panat NA, Maurya DK, Ghaskadbi SS, Sandur SK. Troxerutin, a plant flavonoid, protects cells against oxidative stress-induced cell death through radical scavenging mechanism. Food Chem [Internet]. 2016;194:32-45. doi: 10.1016/j.foodchem.2015.07.078, PMID 26471524.
9. Panat NA, Singh BG, Maurya DK, Sandur SK, Ghaskadbi SS. Troxerutin, a natural flavonoid binds to DNA minor groove and enhances cancer cell killing in response to radiation. Chem Biol Interact [Internet]. 2016;251:34-44. doi: 10.1016/j.cbi.2016.03.024, PMID 27016192.
10. Ping X, Junqing J, Junfeng J, Enjin J. Radioprotective effects of troxerutin against gamma irradiation in mice liver. Int J Radiat Biol [Internet]. 2012;88(8):607-12. doi: 10.3109/09553002.2012.692494, PMID 22571496.
11. Mosmann T. Rapid colorimetric assay for cellular growth and survival: application to proliferation and cytotoxicity assays. J Immunol Methods. 1983;65(1-2):55-63. doi: 10.1016/0022-1759(83)90303-4, PMID 6606682.
12. Tsai CC, Lai TM, Lin PP, Hsieh YM. Evaluation of lactic acid bacteria isolated from fermented plant products for antagonistic activity against urinary tract pathogen *Staphylococcus saprophyticus*. Probiotics Antimicrob Proteins. 2018;10(2):210-7. doi: 10.1007/s12602-017-9302-x, PMID 28780720.
13. Raja Singh P, Arunkumar R, Sivakamasundari V, Sharmila G, Elumalai P, Suganthapriya E, *et al.* Anti-proliferative and apoptosis inducing effect of nimbolide by altering molecules involved in apoptosis and IGF signalling via PI3K/Akt in prostate cancer (PC-3) cell line. Cell Biochem Funct [Internet]. 2014;32(3):217-28. doi: 10.1002/cbf.2993, PMID 23963693.
14. Farooqui A, Khan F, Khan I, Ansari IA. Glycyrrhizin induces reactive oxygen species-dependent apoptosis and cell cycle arrest at G0/G1 in HPV18+ human cervical cancer HeLa cell line [Internet]. Biomed Pharmacother. 2018;97:752-64. doi: 10.1016/j.biopha.2017.10.147, PMID 29107932.
15. Goh H, Kadir HA. *In vitro* cytotoxic potential of Swietenia macrophylla King seeds against human carcinoma cell lines. Vol. 5(8); 2011. J Med Plants Res [Internet]. p. 1395-404 [cited Nov 10 2025]. Available from: http://www.academicjournals.org/JMPR.
16. So EC, Chow LW, Chuang CM, Chen CY, Wu CH, Shiao LR *et al.* MCU-i4, a mitochondrial Ca2+ uniporter modulator, induces breast cancer BT474 cell death by enhancing glycolysis, ATP production and reactive oxygen species (ROS) burst. Oncol Res [Internet]. 2025;33(2):397-406. doi: 10.32604/or.2024.052743, PMID 39866241.
17. Gatti A, Movilia A, Roncoroni L, Citro A, Marinoni S, Brando B. Chronic myeloid leukemia with P190 BCR-ABL translocation and persistent moderate monocytosis: A case report. J Hematol [Internet]. 2018;7(3):120-3. doi: 10.14740/jh421w, PMID 32300425.
18. Gómez-Castañeda E, Hopcroft LE, Rogers S, Munje C, Bittencourt-Silvestre J, Copland M, *et al.* Tyrosine kinase inhibitor independent gene expression signature in CML offers new targets for LSPC eradication therapy. Cancers (Basel). 2022;14(21):5253. doi: 10.3390/cancers14215253, PMID 36358672.
19. Calabretta B, Perrotti D. The biology of CML blast crisis. Blood. 2004;103(11):4010-22. doi: 10.1182/blood-2003-12-4111, PMID 14982876.
20. González-Vallinas M, González-Castejón M, Rodríguez-Casado A, Ramírez de Molina A. Dietary phytochemicals in cancer prevention and therapy: a complementary approach with promising perspectives. Nutr Rev [Internet]. 2013;71(9):585-99. doi: 10.1111/nure.12051, PMID 24032363.
21. Abotaleb M, Samuel SM, Varghese E, Varghese S, Kubatka P, Liskova A, *et al.* Flavonoids in cancer and apoptosis. Cancers. 2018;11(1):28. doi: 10.3390/cancers11010028, PMID 30597838.
22. Chirumbolo S, Bjørklund G, Lysiuk R, Vella A, Lenchyk L, Upyr T. Targeting cancer with phytochemicals via their fine tuning of the cell survival signaling pathways. Int J Mol Sci. 2018;19(11):3568. doi: 10.3390/ijms19113568, PMID 30424557.
23. Panche AN, Diwan AD, Chandra SR. Flavonoids: an overview. J Nutr Sci. 2016;5:e47. doi: 10.1017/jns.2016.41, PMID 28620474.
24. Hassanshahi J. Mirzahosseini-pourranjbar A, Hajializadeh Z, Kaeidi A. Anticancer and cytotoxic effects of troxerutin on HeLa cell line: an *in vitro* model of cervical cancer. Mol Biol Rep [Internet]. 2020;47(8):6135-42.
25. Simon HU, Haj-Yehia A, Levi-Schaffer F. Role of reactive oxygen species (ROS) in apoptosis induction. Apoptosis. 2000;5(5):415-8. doi: 10.1023/A:1009616228304, PMID 11256882.
26. Allegra A, Mirabile G, Caserta S, Stagno F, Russo S, Pioggia G, *et al.* Oxidative stress and chronic myeloid leukemia: A balance between ROS-mediated pro- and anti-apoptotic effects of tyrosine kinase inhibitors. Antioxidants (Basel). 2024;13(4):461. doi: 10.3390/antiox13040461, PMID 38671909.
27. Saraei R, Marofi F, Naimi A, Talebi M, Ghaebi M, Javan N, *et al.* Leukemia therapy by flavonoids: future and involved mechanisms. J Cell Physiol. 2019;234(6):8203-20. doi: 10.1002/jcp.27628, PMID 30500074.
28. Habibi A, Davari A, Isazadeh K. A novel LL-37@NH2@Fe3O4 inhibits the proliferation of the leukemia K562 cells: *in vitro* study. Sci Rep [Internet]. 2024;14(1):22245. doi: 10.1038/s41598-024-71946-7, PMID 39333586.
29. Scott MT, Liu W, Mitchell R, Clarke CJ, Kinstrie R, Warren F, *et al.* Activating p53 abolishes self-renewal of quiescent leukaemic stem cells in residual CML disease. Nat Commun. 2024;15(1):651. doi: 10.1038/s41467-024-44771-9, PMID 38246924.
30. Hollstein M, Sidransky D, Vogelstein B, Harris CC. p53 mutations in human cancers. Science. 1991;253(5015):49-53. doi: 10.1126/science.1905840, PMID 1905840.
31. Vogelstein B, Kinzler KW. p53 function and dysfunction. Cell. 1992;70(4):523-6. doi: 10.1016/0092-8674(92)90421-8, PMID 1505019.
32. Yan Y, Tao H, He J, Huang SY. The HDOCK server for integrated protein-protein docking. Nat Protoc. 2020;15(5):1829-52. doi: 10.1038/s41596-020-0312-x, PMID 32269383.

Cite this article: Almasoudi HH. Unveiling Novel Insights in Chronic Myeloid Leukemia Cell Lines K562 through *in vitro* and *in silico* Approach Targeting of Apoptosis and Oxidative Stress Pathways. Indian J of Pharmaceutical Education and Research. 2026;60(1s):s358-s370.